

# THE STUDY OF HIGH TEMPERATURE OXIDATION BY SURFACE ANALYTICAL TECHNIQUES

C. A. C. Sequeira<sup>(1)\*</sup>, Y. Chen<sup>(2)</sup>, D. M. F. Santos<sup>(1)</sup> and X. Song<sup>(2)</sup>

Artigo submetido em Julho de 2007 e aceite em Janeiro de 2008

## ABSTRACT

Surface analytical techniques represent a powerful arsenal for practical surface analysis. Here it is shown how the classical techniques are applied to study high temperature oxidation of metals, facilitating the description of the oxidation process and indicating ways to reduce oxidation.

**Keywords:** High Temperature Oxidation, Auger Electron Spectroscopy, X-ray Photoelectron Spectroscopy, Secondary Ion Mass Spectrometry

# ESTUDO DA OXIDAÇÃO A ALTA TEMPERATURA POR TÉCNICAS DE ANÁLISE SUPERFICIAL

## RESUMO

As técnicas de análise superficial representam um poderoso arsenal para a análise prática de superfícies. Neste artigo, mostra-se como se empregam as técnicas clássicas no estudo da oxidação de metais a alta temperatura, facilitando a descrição do processo de oxidação e indicando formas de a reduzir.

**Palavras Chave:** Oxidação a Alta Temperatura, Espectroscopia de Electrões Auger, Espectroscopia Fotoelectrónica de Raios X, Espectrometria de Massa de Iões Secundários.

## 1. INTRODUCTION

In recent years, the problem of high temperatures in relatively complex environments such as mixed gases with low oxygen activities but significant carbon or sulphur activities, or environments in which gases and liquids (molten salts) intervene on the alloy surface, has become of much greater importance [1-6]. The term high temperature oxidation, here, refers to material degradation (corrosion) at temperatures higher than the ambient temperatures, when exposed to hostile gaseous environments.

The rate of attack is controlled by many factors including temperature, pressure, nature of corroding species, composition of materials, etc. The attack is invariably initially very fast but may then slow down because a protective layer is formed between the surface and the gas/liquid. Some layers protect better than others and it is the job of the scientist to improve the protective nature of the layer. To do this, it is important that the initial reaction between the corroding molecules and the surface can be identified and that the succeeding layers be well characterised. Surface analytical techniques have been attempting to do this for more than forty years [7]. Initially, Low Energy Electron Diffraction (LEED) [8] was used to determine surface structures and this was supplemented, in 1968, by Auger Electron Spectroscopy (AES) [9,10] and X-ray Photoelectron Spectroscopy (XPS) [9] which identified surface atoms and

their chemical state. In the eighties, Secondary Ion Mass Spectrometry (SIMS) [11-13] has been used to detect trace element additions in the surface layers. Through the 1990's, there has been a rapid proliferation of surface analytical techniques but, for the present time, these novel techniques have been mainly used for researchers and expert areas [14-16].

In this paper, an attempt will be made to show how three of the most widely used techniques, LEED-AES, XPS and SIMS, are applied to the study of oxidation, to indicate how models may be devised to reduce degradation by high temperature oxidation.

## 2. SURFACE ANALYTICAL TECHNIQUES

### 2.1 Auger and Photoelectron Spectroscopy

These processes, described in detail elsewhere [5], are schematically illustrated in Fig. 1. In both techniques, a surface atom is ionised by removal of an inner shell electron. In XPS ionisation, this is achieved by bombarding the surface with photons with energies between 1-2 keV. The resulting photoelectron has an energy given by:

$$E = h\nu - E_k \quad \text{Eq. 1}$$

<sup>(1)</sup> Instituto Superior Técnico, Av. Rovisco Pais, 1, 1049-001 Lisboa, Portugal

<sup>(2)</sup> University of Wisconsin, 1500 Engineering Drive, Madison 53706, USA, e-mail: chen2@wisc.edu

\* A quem a correspondência deve ser dirigida, e-mail: cesarsequeira@ist.utl.pt

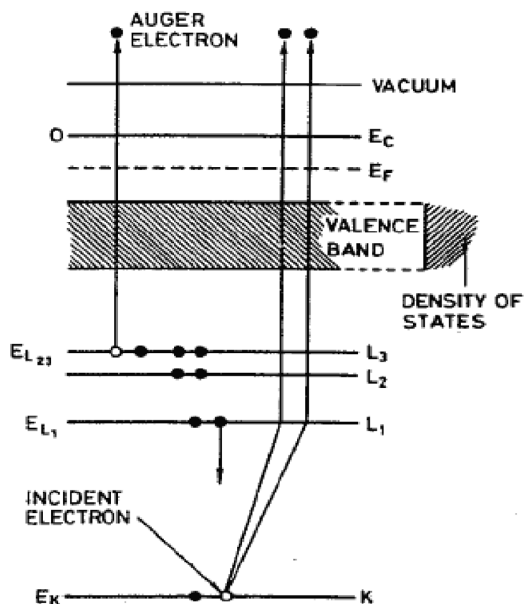


Fig. 1 – Schematic representation of the Auger process.

The energy of the photoelectron is measured using a concentric hemispherical analyser. Typically the energy can be measured to an accuracy of ± 0.1 eV. Knowing the energy of the incident photon, the binding energy of the electron in the atom can be determined. In addition, changes in binding energy that occur when elements combine together can be detected and the chemical state of the atom identified.

In AES, ionisation is produced by bombarding the surface with electrons with energies from 2-15 keV. When an electron is ejected from an inner shell (K shell) of an atom the resultant vacancy is soon filled by an electron from one of the outer shells (L). This releases energy, which may be transferred to another outer electron (L shell), which is ejected. The energy of the Auger electron is given by:

$$E_{\text{Auger}} = E_K - E_{L_1} - E_{L_{2,3}} \quad \text{Eq. 2}$$

The energy of the Auger electron is measured by either hemispherical or cylindrical analysers. The former has

better energy resolution and hence gives chemical state information while the latter has a higher transmission function and is useful for kinetic studies.

XPS has the advantage that it can give reliable chemical state information but has limited spatial resolution, while AES has excellent spatial resolution (10 nm) but limited chemical state.

## 2.2 Secondary Ion Mass Spectrometry

In this technique [9], a beam of ions impinges on the surface under examination, ejecting ions and ion clusters from the surface which are then detected and mass analysed. The incident ion probe can vary from diffuse low energy inert ions to high energy fine focus ions from liquid metal sources. The ejected ions are detected by electrostatic, magnetic or time of flight mass spectrometers. Clearly this technique is destructive, although sensitive detectors reduce this to negligible levels, but it is capable of detecting very small concentrations in surface layers.

## 3. OXIDE CHARACTERISATION

### 3.1 Initial Stages and Thin Films

It is important to identify the nature of the oxide that forms initially. In this respect, both XPS and AES are useful. Fig. 2 shows the oxygen 1s peak during the initial stages of exposure of nickel to oxygen at room temperature and then the effect of heating on this oxide [17]. Initially undissociated oxygen is detected (Stage 1) which then dissociates forming a layer of dissociated and undissociated oxygen on the top of the nickel metal (Stage 2). Oxygen then diffuses into the nickel (Stage 3) which may be slow at room temperature but as the temperature is increased so the speed of the reaction increases. By determining the temperature at which this diffusion occurs from the O 1s peak shift the activation energy for diffusion can be determined.

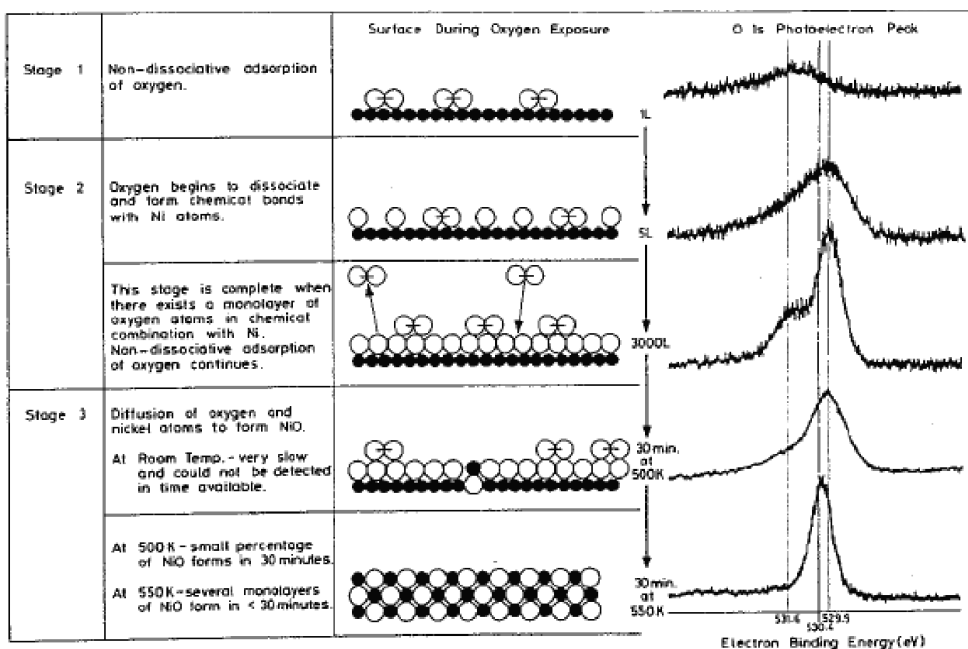


Fig. 2 – Changes in the oxygen O 1s peak during oxidation of nickel [17].

In binary and ternary alloys, the oxide which first forms is determined by the temperature and rate of arrival of the gas atoms. Fig. 3 shows spectra from stainless steel exposed to low oxygen pressure at room temperature and 873 K. At room temperature, the initial oxide is an iron rich spinel of the form  $Fe_3O_4$  but, at high temperature and low gas pressure, the chromium rich rhombohedral oxide  $Cr_2O_3$  is able to form.

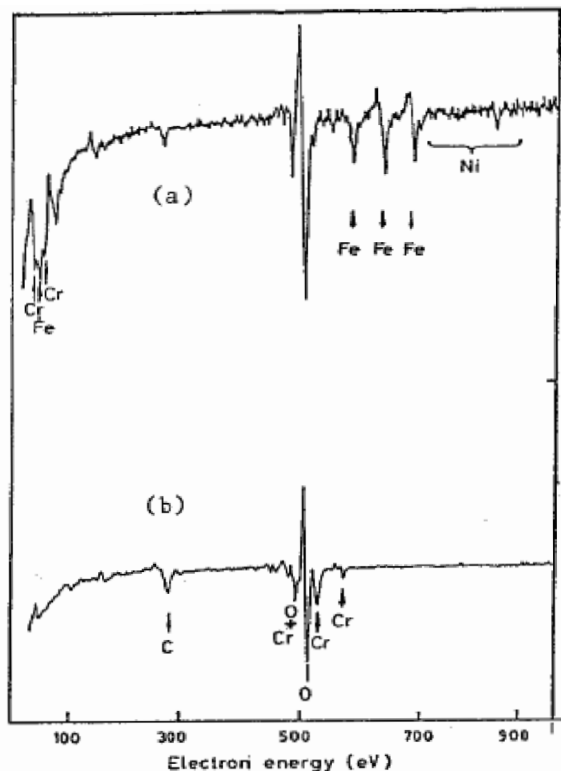


Fig. 3 – Auger spectra from stainless steel exposed to a low oxygen pressure; (a) Room temperature (b) 873 K.

Elements present in the bulk in very small quantities can have a dramatic effect on the initial oxidation. Sulphur is present in austenitic steels at a level of approximately 200 ppm. At temperatures of 500 °C and above the sulphur diffuses to the surface where it reacts with the impinging gas atoms to form  $SO_2$  which is released into the environment [18]. Fig. 4 shows the surface composition of a stainless steel, determined using AES, as a function of time exposed to  $10^{-5}$  Pa oxygen at 873 K. Initially the surface has a high concentration of sulphur present but this is gradually reduced by reaction with oxygen. It is only when the sulphur has been effectively removed from the bulk that the surface oxide can form. It then does this by forming the rhombohedral  $Cr_2O_3$  but almost immediately manganese is incorporated into this oxide forming the spinel oxide  $MnCr_2O_4$ .

### 3.2 High Pressure Oxidation

#### 3.2.1 *In situ* studies

There is little problem in following the surface composition as a function of exposure time at low gas pressures but at high pressures the sample cannot be analysed directly but must be transferred from the corrosive environment to the ultra high vacuum of the spectrometer. In general, it is necessary to stop the experiment and transfer the sample at room temperature. This causes problems in that the surface can become contaminated during transfer and cooling down may result in compositional changes. Contamination can be avoided by incorporating a high pressure cell in the vacuum system while transfer can be achieved by simply evacuating the high pressure cell. An example of the corrosion of a 9% chromium steel in  $CO_2$  at 873 K at one atmosphere is shown in Fig. 5 [19]. Initially, the sulphur which segregates to the surface is reduced to approximately 7 at. % while at the

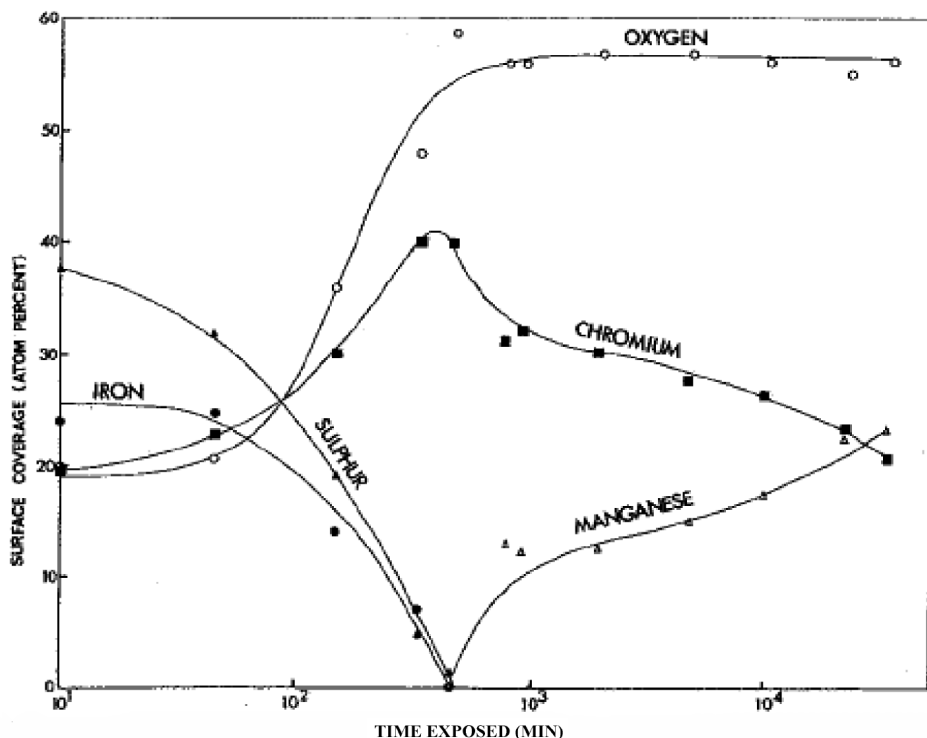


Fig. 4 – Surface composition of stainless steel during exposure to  $10^{-5}$  Pa oxygen at 873 K [18].

same time carbon rises to approximately 10 at. %. Chromium also disappears from the surface and is not detected in the surface oxide for the remainder of the experiment in contrast to the low pressure oxidation. The composition of the surface remains constant from 10 minutes exposure to 1000 minutes when the sulphur and carbon cease to be detected and the

oxygen level increases. These compositional variations can be explained as sulphur first diffusing to the oxide/metal interface and then diffusing across the oxide at a slower rate. The sulphur may act to fix carbon from the  $\text{CO}_2$  and this would explain the simultaneous disappearance of these elements.

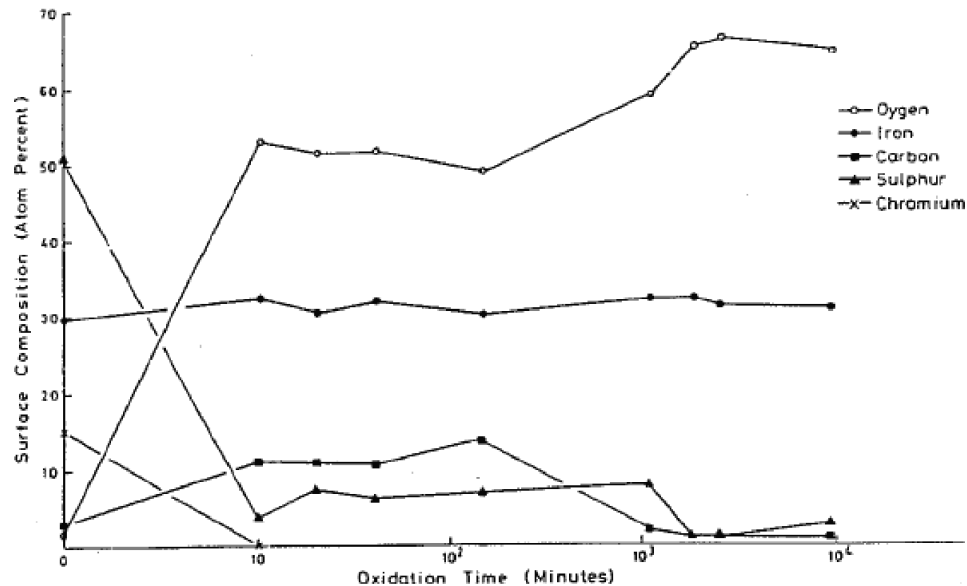


Fig. 5 – Surface composition of 9% Cr steel exposed to 1 atmosphere of  $\text{CO}_2$  at 873 K [19].

### 3.2.2 Oxide characterisation

Information on the oxidation process can be deduced by following the surface composition during oxidation but this only gives part of the information required. Changes are taking place within the oxide which needs to be identified. It is possible to obtain some qualitative information on the compositional changes as a function of depth in a nondestructive manner by using the changes in electron escape depths as a function of energy [20]. This may be supplemented by bulk techniques such as X-ray fluorescence spectroscopy (XRF) [21] and X-ray Diffraction (XRD) [22]. However, in most cases it is necessary to destroy the sample

to get the required depth information. The most commonly employed method is ion depth profiling accompanied by AES or XPS. One such depth profile is reproduced in Fig. 6. This is a profile through an oxide formed on 20% Cr / 25% Ni/Nb stabilised steel following oxidation in  $\text{CO}_2$  at 1 atmosphere pressure and 1123 K for 200 hours [23]. From this profile, it can be seen that the oxide is composed of two separated layers. The outer layer, approximately 0.5 micrometers thick, is composed of chromium and manganese while the inner layer, also 0.5 micrometers thick, is essentially a chromium oxide. X-ray diffraction confirmed that the outer layer was a spinel oxide  $\text{MnCr}_2\text{O}_4$  and the inner layer rhombohedral  $\text{Cr}_2\text{O}_3$ .

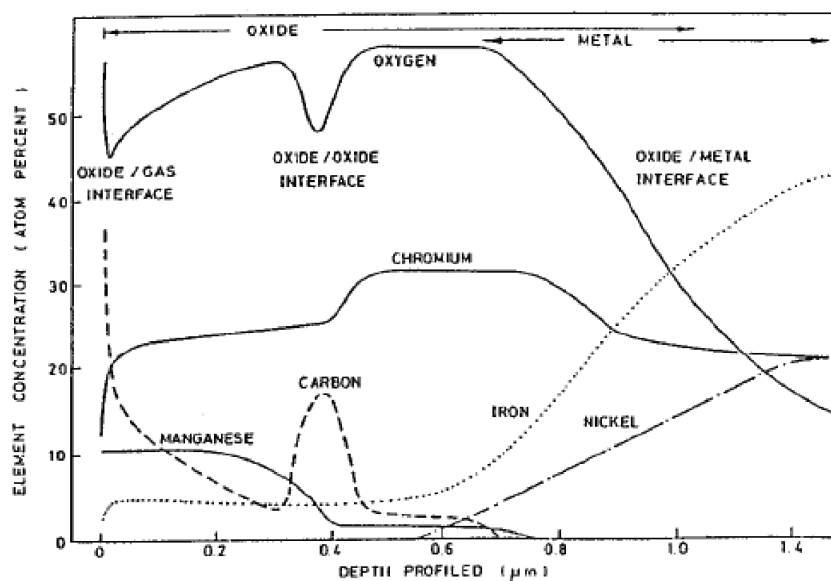
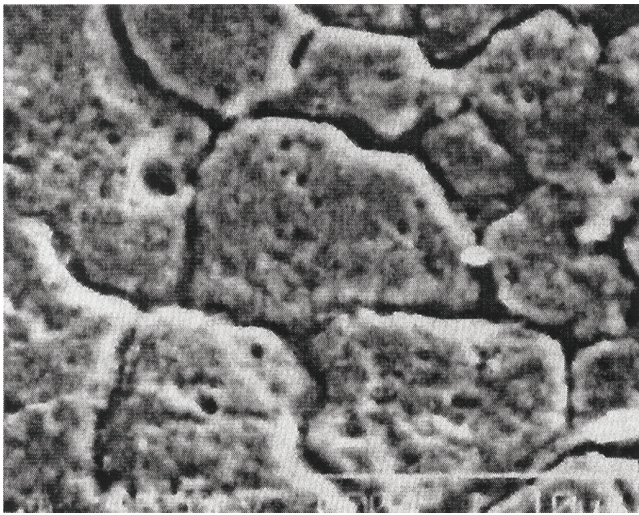
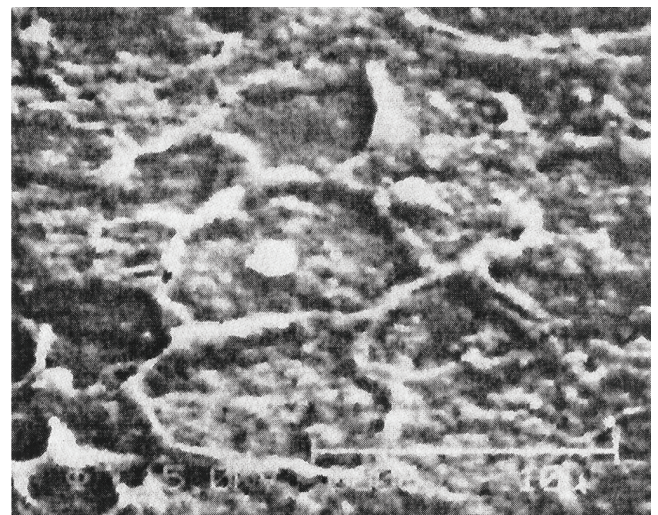


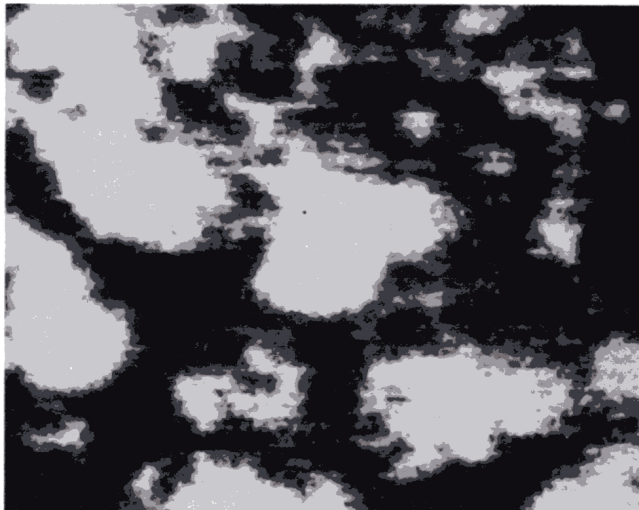
Fig. 6 – Depth profile through the oxide formed on 20% Cr / 25% Ni/Nb steel in 1 atmosphere of  $\text{CO}_2$  at 1123 K [23].



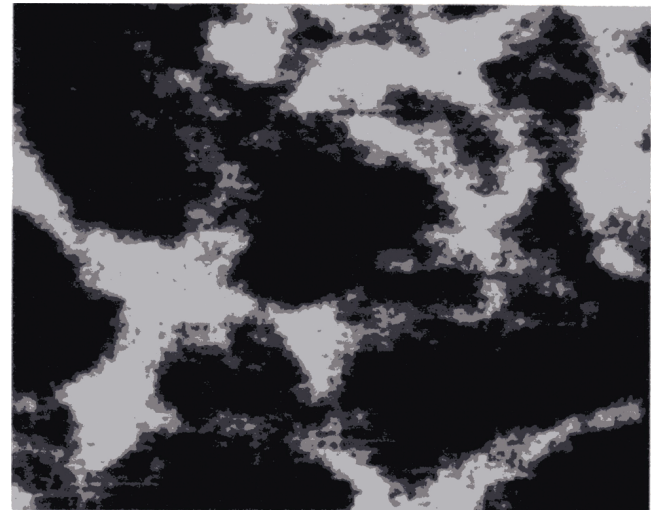
(a) Electron image metal side



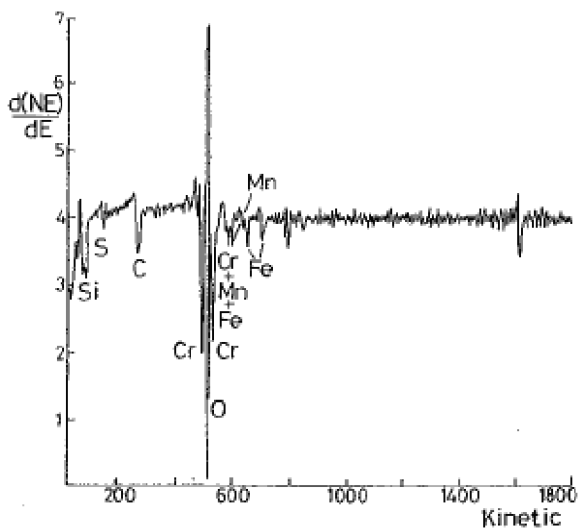
(b) Electron image oxide side



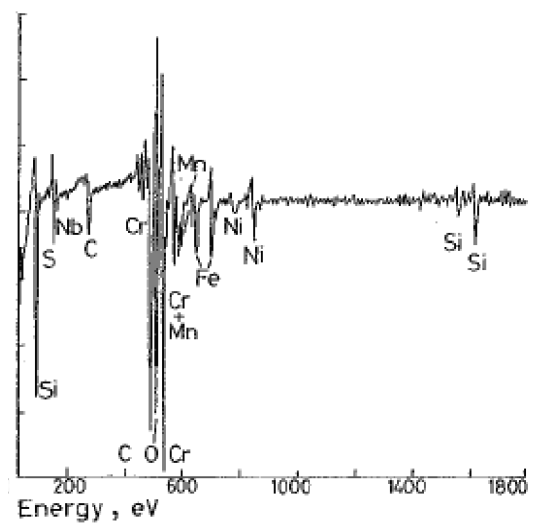
(c) Auger Chromium map metal side



(d) Auger Iron map metal side



(e) Auger spectrum from grain boundary region



(f) Auger spectrum from surface at grain centre

Fig. 7 – Surface analysis of the metal/oxide interface on 20% Cr / 25% Ni/Nb steel [27].

Depth profiling is very useful but the resolution degrades with depth profile and deeply buried interfaces may not be detected, particularly for the metal/oxide interface. This may be the site of thin layers of material which can have a marked influence on the oxidation process. The interface may be accessed in a number of ways. For example, taper sections through the oxide may be produced by polishing and the contaminated layer removed by ion etching [24]. This produces a magnified cross section of the oxide and thin layers may be identified by analysing at points along the taper. A variant on this technique is known as Ball Cratering [25] in which a shallow crater is produced in the oxide by polishing with a rotating hard sphere. Another technique which has proved successful in several laboratories is Sputter Ion Plating (SIP) [26]. Here the oxide is stripped from the metal revealing two sides of the interface. The oxide is coated with a metal layer at 500 K, typically nickel or molybdenum, while sputtering in a plasma discharge. This produces a strong bond between the coated layer and the oxide. On cooling, the stresses which are set up between the coat and the oxide cause the oxide to fracture at its weak point and peel away from the metal substrate [27]. This technique will always expose the weakest interface which may not necessarily be the oxide/metal interface. Fig. 7 shows the metal and oxide sides of the interface on 20% Cr / 25% Ni/Nb steel following oxidation at 837 K in 40 atmospheres of CO<sub>2</sub> for 12000 h. Fig. 7a is an electron image from the metal side while Fig. 7b is from the oxide side. Auger element maps from the metal side for chromium and iron are reproduced as Figs. 7c and 7d, respectively. While Auger spectra from the grain boundary and grain centre are reproduced as Figs. 7e and 7f. From this type of data, together with additional depth profiling, it was possible to deduce that a layer of silicon, 20 nanometres thick, forms at the metal oxide interface. When the oxide is stripped off fracture occurs through this layer at the grain centres but at grain boundaries the fracture path is through the chromium oxide overlying the thin silica layer.

### 3.3 Development of Models

The objective of surface studies involving corrosion or oxidation is to develop models to describe the oxidation process and to devise methods which may improve the corrosion resistance. In this section, we shall give an example showing how results of the type obtained above can be used to predict and improve corrosion resistance in steels.

#### 3.3.1 Initial oxide

As shown above, the development of the initial oxide is dependent on a number of factors. These include gas pressure, temperature, alloy composition and trace element impurities. The first formed oxide will be controlled by the rate of arrival of the gas atoms and the jump frequency of the atoms in the alloy. If the rate of arrival is slow compared to the atom jump frequency, then the first formed oxide will be that of the most thermodynamically stable oxide. In the case of iron-chromium-nickel alloys this will be a chromium oxide. However, if the rate of arrival is fast compared to the jump

frequency, then the first formed oxide will have a metal cation content similar to the alloy matrix. Then, the oxide is controlled by the rate of transport of cations across this layer. In the case of iron-chromium-nickel alloys, iron diffuses much faster and the oxide rapidly becomes an iron rich spinel. This is shown in Fig. 8 for 20% Cr / 25% Ni/Nb steel [28]. Here, jump frequencies deduced from experiments involving nickel have been used to predict the first formed oxide under a variety of conditions. Good agreement is obtained between prediction and experiment.

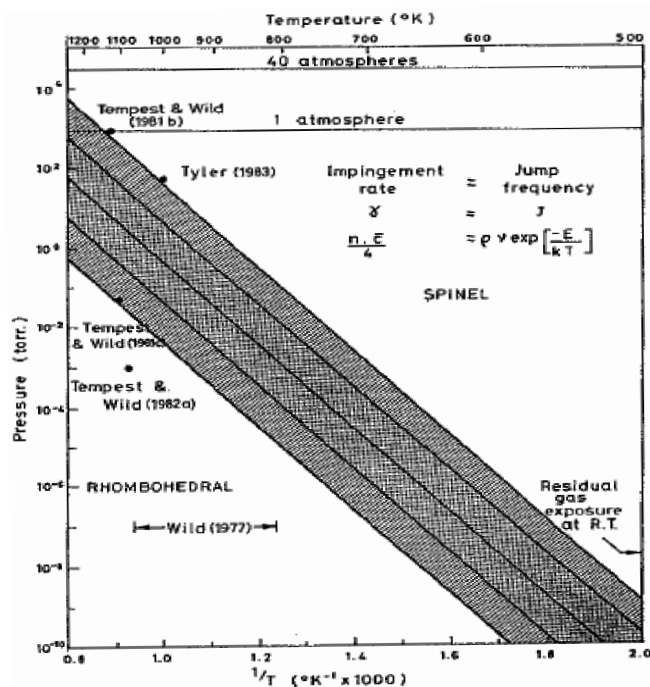


Fig. 8 – Prediction of oxide formation on stainless steel [28]

#### 3.3.2 Subsequent oxides

Once the oxide has formed, then the growth rates will be controlled by rates of transport of cations or anions across the oxide. Only in a few limited cases does the gas arrival rate control oxidation. As the oxide thickens so the flux of cations across the oxide decreases and reactions occurring within the oxide and at the oxide/metal interface become important. In particular in the iron-chromium-nickel system, chromium gradually reduces the iron oxide, which forms at high pressure, first to an iron-chrome spinel of the type FeCr<sub>2</sub>O<sub>4</sub> and then to the rhombohedral Cr<sub>2</sub>O<sub>3</sub>. Transport of cations across the rhombohedral layer is much slower than across the spinel and so the chromium oxide acts to protect the steel by reducing the oxidation rate. Two other elements influence the nature of the oxide. These are manganese and silicon, which are present in the alloy in less than 1-2 wt. %. Manganese has a very fast rate of diffusion through the oxide and is thermodynamically more stable than iron and comparable to chromium. For this reason, it rapidly becomes incorporated in the outer oxide layers of both iron and chromium oxides to levels of up to 10 at. %.

Silicon influences the oxidation process at the metal oxide interface [29,30,31]. Silicon is thermodynamically more stable than chromium oxide. It therefore reduces the protective  $\text{Cr}_2\text{O}_3$  to  $\text{SiO}_2$  and this forms a very thin amorphous layer below the other oxides. Silica also acts to reduce the oxidation rates by allowing cation diffusion.

### 3.3.3 Influence of trace elements

Trace elements can modify the oxidation process considerably. In particular, sulphur, which is present in most stainless steels in concentrations of less than 200 ppm, will modify the oxidation. Sulphur diffuses to the surface where it reacts with the oxidising gas to form  $\text{SO}_2$  which is released to the environment. This effectively reduces the pressure of the corroding gas and can, in turn, influence the role of manganese which is present in stainless steels and acts, with nickel, to stabilise the austenitic phase. It is a highly volatile element and is lost from a stainless steel by effusion at temperatures above 700 K [32]. However, the phenomenon only occurs in the absence of a surface oxide and thus the sulphur, in reducing the oxide, is also allowing the manganese to be lost. This can have the effect of allowing ferrite to form, particularly near the surface, with consequences for the mechanical properties.

### 3.3.4 Pretreatments

Clearly certain oxides offer more protection against the corrosive environment than others. By creating condi-

tions in which these oxides form, it is possible to reduce the alloy loss during oxidation. In the case of 20% Cr / 25% Ni/Nb steel, the protective oxide is the rhombohedral  $\text{Cr}_2\text{O}_3$ . This forms on this particular alloy at high temperatures and low oxygen potentials and it is therefore possible to produce conditions in which it will form. This has been done by adding water vapour to hydrogen during alloy annealing at 1373 K [33] and by heating to 1023 K at low pressure of  $\text{CO}_2$  [34]. Both pretreatments produce the chromium-rich oxide, though with manganese incorporation, and both offer protection to corrosion, particularly at temperatures below 973 K. Fig. 9 shows the weight gain of 20% Cr / 25% Ni/Nb steel oxidised in 40 atmospheres of  $\text{CO}_2$  at 823 K for both untreated and preoxidised material. This is clearly an improvement in corrosion resistance of a factor of three to four.

## 4. CONCLUSIONS

Surface analytical techniques are ideally suited to the study of corrosion processes. It is possible to follow the oxidation from the formation of the first few atom layers to the development of micrometer thick oxides. The oxide can be completely characterised by combining surface analysis with depth profiling and other specialised techniques [35-37]. Information gained from these studies allows predictions to be made which identify the oxide that forms under a given set of conditions. How the oxide grows can also be studied and procedures can be developed to produce oxides which offer improved oxidation resistance [38-39].

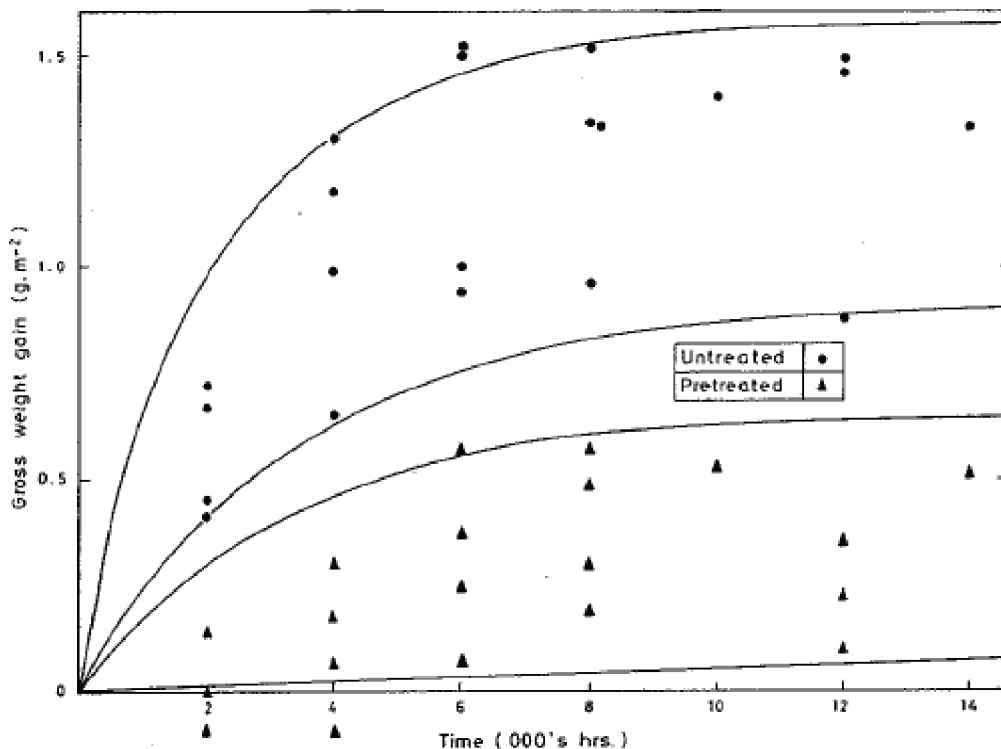


Fig. 9 – Weight gain of preoxidised and untreated 20% Cr / 25% Ni/Nb steel oxidised at 823 K in  $\text{CO}_2$  [34].

## REFERENCES

- [1] G. BONNET, J. M. BROSSARD and J. BALMAIN, *Mater. Corros.*, 56, 12, 942 (2005).
- [2] K. FUJITA, *Surf. Coat. Technol.*, 196, 1-3, 139 (2005).
- [3] B. SAUERHAMMER, D. SENK, E. SCHMIDT *et al.*, *Metall. Mater. Trans. B*, 36, 4, 503 (2005).
- [4] P. E. GANNON *et al.*, *Surf. Coat. Technol.*, 188-189, 1-3, 55 (2004).
- [5] R. HAUGSRUD, *Corros. Sci.*, 45, 6, 1289 (2003).
- [6] M. FUKUMOTO *et al.*, *J. Jpn. Inst. Met.*, 66, 7, 684 (2002).
- [7] M. J. GRAHAM, *Mater. Sci. Forum*, 522-523, 61 (2006).
- [8] G. Y. LAI (High Temperature Corrosion and Materials Applications), ASM International, Materials Park, USA (2007).
- [9] J. F. WATTS and J. WOLSTENHOLME (An Introduction to Surface Analysis by XPS and AES), 2<sup>nd</sup> ed., Wiley, USA (2003).
- [10] M. PRUTTON and M. M. EL GOMATI (Scanning Auger Electron Microscopy), 1<sup>st</sup> ed., Wiley, USA (2006).
- [11] H.W. WERNER, *Surf. Interface Anal.*, 2, 56 (1980).
- [12] A. BENNINGHOVEN, F. D. ANDENAU and H.W. WERNER (Secondary Ion Mass Spectrometry), Wiley & Sons, New York, USA (1987).
- [13] J. H. GROSS (Mass Spectrometry: A Textbook), 2<sup>nd</sup> ed., Springer, Germany (2006).
- [14] S. B. NEWCOMB and J. A. LITTLE, (Microscopy of Oxidation 3), The Institute of Materials, London, UK (1997).
- [15] G. TATLOCK and S.B. NEWCOMB, Eds. (Microscopy of Oxidation 4) *Sci. Rev.*, 17, 1 (2000).
- [16] G. TATLOCK and S.B. NEWCOMB, Eds. (Microscopy of Oxidation 5) *Sci. Rev.*, 20, 1 (2003).
- [17] G. C. ALLEN, P. M. TUCKER and R. K. WILD, *Oxid. Met.*, 13, 223 (1979).
- [18] R. K. WILD, *Corros. Sci.*, 17, 87 (1977).
- [19] G. C. ALLEN, I. T. BROWN and R. K. WILD, *Oxid. Met.*, 12, 83 (1978).
- [20] H. R. VERMA (Atomic and Nuclear Analytical Methods: XRF, Mössbauer, XPS, NAA and Ion-Beam Spectroscopic Techniques), 1<sup>st</sup> ed., Springer, Germany (2007).
- [21] B. BECKHOFF *et al.*, (Handbook of Practical X-Ray Fluorescence Analysis), 1<sup>st</sup> ed., Springer, Germany (2006).
- [22] R. GUINEBRETIERE (X-Ray Diffraction by Polycrystalline Materials), ISTE Publishing Company, London, UK (2007).
- [23] P. A. TEMPEST and R. K. WILD, *J. Nucl. Mat.*, 102, 183 (1981).
- [24] M. PISAREK, *Ann. Chim. - Sci. Mat.*, 32, 4, 383 (2007).
- [25] M. G. GEE *et al.*, *Wear*, 255, 1-6, 1 (2003).
- [26] V. RIGATO *et al.*, *Surf. Coat. Technol.*, 131, 1-3, 206 (2000).
- [27] G. C. ALLEN, R.K. WILD and M. WEISS, *Phil. Mag.*, 48, 373 (1983).
- [28] P. A. TEMPEST and R. K. WILD, *Oxid. Met.*, 23, 207 (1985).
- [29] H. E. EVANS and A.T. DONALDSON, *Oxid. Met.*, 50, 457 (1998).
- [30] J. S. DUNNING, D.E. ALMAN and J.C. RAWERS, *Oxid. Met.*, 57, 409 (2002).
- [31] A. PAUL, R. SANCHEZ, O. M. MONTES *et al.*, *Oxid. Met.*, 67, 87 (2007).
- [32] F. H. STOTT *et al.*, *Wear*, 186-187, 1, 291 (1995).
- [33] X. VANDEN EYNDE, J. P. SERVAIS and M. LAMBERIGTS, *Surf. Interface Anal.*, 35, 12, 1004 (2003).
- [34] P. A. TEMPEST and R. K. WILD, *Oxid. Met.*, 30, 209 (1988).
- [35] N. BIRKS, G. H. MEIER and F. S. PETTIT (Introduction to the High Temperature Oxidation of Metals) Cambridge University Press, Cambridge, UK (2006).
- [36] A. S. KHANNA (Introduction to High Temperature Oxidation and Corrosion) ASM International, Materials Park, USA (2002).
- [37] P. KOFSTAD (High Temperature Corrosion) Elsevier Applied Science Publishers, London, UK (1988).
- [38] V. LEVITIN (High Temperature Strain of Metals and Alloys: Physical Fundamentals) 1<sup>st</sup> ed., Wiley-VCH, Weinheim (2005).
- [39] M. SCHÜTZE (Protective Oxide Scales and their Breakdown) John Wiley, Chichester, UK (1997).